Original article

Using gradient origamis to pre-program curvatures

Reza Hedayati[1,*], Nima Roudbarian[2], Sara Tahmasiyan[2]

[1]Department of Aerospace Structures and Materials, Faculty of Aerospace Engineering, Delft University of Technology (TU Delft), Kluyverweg 1, 2629 HS, Delft, The Netherlands

[2]School of Mechanical Engineering, College of Engineering, University of Tehran, Tehran, Iran.

*Corresponding author, Email: rezahedayati@gmail.com

Abstract

Origami structures are a traditional Japanese art which have recently found their way into engineering applications due to their powerful capability to transform flat 2D structures into complex 3D structures along their creases. Here, gradient Miura-ori origamis are introduced as a method to pre-program out-of-plane curvatures. Nine types of unit cell distributions in the origami lattice structure including checkered, linear gradient, concave radial gradient, convex radial gradient, and striped have been considered. These distributions of Miura-ori origami can create twisting, saddling, bending, local inflation, and wavy shapes, as well as their combinations when the origami lattice structure is loaded in compression/tension.

Keywords: Origami; Gradient, Miura-Ori; Metamaterials; Curvature

Designer materials, where rationally designed geometry at the small-scale gives rise to unusual materials properties at the macro-scale, are often called metamaterials [1, 2]. Origami structures are a traditional Japanese art which have recently found their way into engineering applications due to their powerful capability to transform flat 2D structures into complex 3D structures along their creases. Particularly, Miura-ori origami, also known as herringbone geometry (Figure 1), has been proposed as an origami-based mechanical metamaterial [3]. This design was first invented to pack solar panels efficiently, but it is relevant to note that this pattern also occurs in natural structures such as leaves, embryonic intestine [4], and vertebrate guts [5]. The mathematical richness and tunability of Miura-ori geometry allows using it in different scales from nanometric level to architecture [6]. The suitability of Miura-ori for engineering applications lies in its four spectacular characteristics: being able to be folded rigidly, having only one degree of freedom, having negative Poisson's ratio, and being flat-foldable [6].

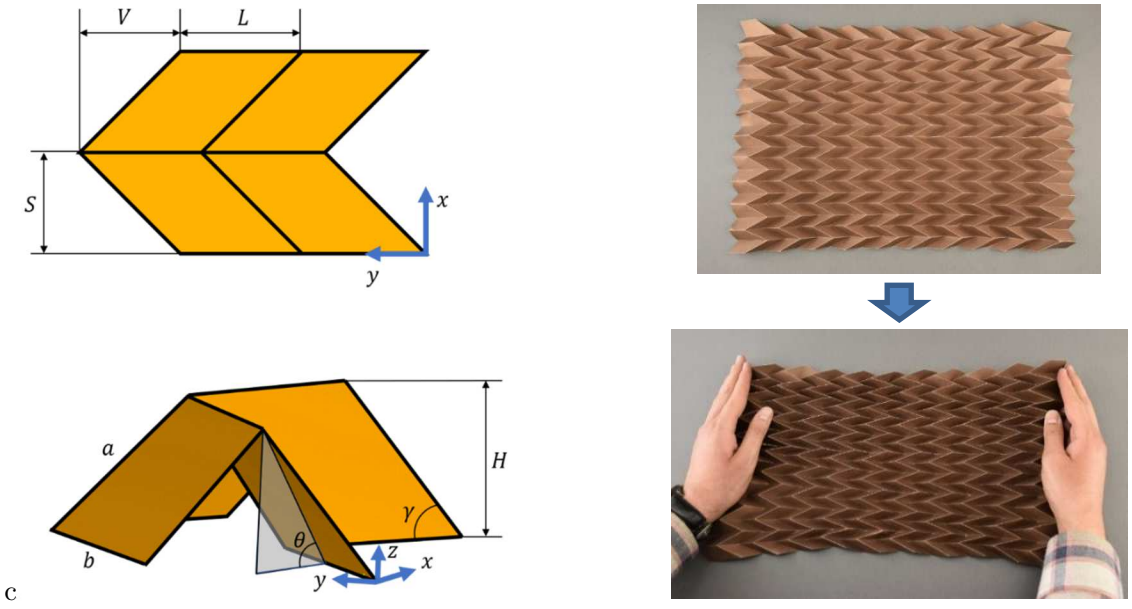

(a) (b)

Figure 1: (a) Geometry and dimensions of unit cells of a Miura-ori origami structure, (b) Miura-ori origami with uniform unit cell distribution before and after compression

3D exotic materials with negative Poisson's ratio (known as auxetics) offer extreme mechanical properties such as high shear resistance, energy absorption, indentation resistance, and toughness [7]. When used in 2D setting, a structure with spatially incompatible auxetic properties can create various 3D shapes through out-of-plane buckling [8].

Given the richness of the Miura-ori origami, the question that arises here is whether or not it is possible to create basic well-known Euclidean and non-Euclidean 3D curvatures using Miura-ori tessellations upon application of an external stimulus such as mechanical load. There has been a few studies which have used origami tessellations to create pre-programed (not necessarily 3D) curvatures [3, 6, 9]. Although a recent study presented an optimization-based method procedure to produce Miura-ori tessellations [6] programmed to create 3D geometries with some approximations, no study has been carried out on how basic gradient distributions of Miura-ori unit cells can be used to create various basic 3D curvatures. Basic Miura-ori distributions (rather than ones created by numerical models) have the advantages of being easy to understand and thus easy to implement for practical problems.

In this paper, for the first time, we introduce basic gradient tessellations as a tool to create programmable basic 3D curvatures. In our previous work [10], we demonstrated how using gradient distributions of re-entrant auxetics can lead to action-at-a-distance actuators. While such block-shaped actuators are useful in many applications such as soft robotics, sensors, and controllers [10], curved actuators seem to offer more exciting functionalities useful in more advanced configurations.

Geometries

Eight types of tessellations with variable mountain height namely checkered, linear gradient (in both the X and Y directions), concave radial gradient, convex radial

gradient, striped (in both the X and Y directions), and regular were considered. It must be noted that the XY is the plane parallel to the mid-plane of the origami lattice structure (see Figure 1a). In most of the structures, regardless of the mountain peak height, the parameters S, L, and V were set constant and equal to $S = 19.64$ mm, $L = 19.84$ mm, and $V = 22.68$ mm. The overall length of the origami lattice structures in each direction was therefore 392.7 mm. The maximum and minimum heights of the mountains in all the configurations was considered as $H_{max} = 22.5$ mm and $H_{min} = 4.5$ mm, respectively. Some of the above-mentioned geometries, due to including non-flat surfaces, or due to including particular patterns were not possible to be manufactured by folding flat plates. Therefore, to make the origamis foldable from flat papers, in addition to the noted structures, two additional geometries (linear X and striped X) in which instead of mountain height, unit cell width was varied was also considered. The dimensions of Miura-origami are [11]:

$$a = \sqrt{L^2 + H^2} \tag{1}$$

$$\theta = \sin^{-1}\left(\frac{H}{a\ sin(\gamma)}\right) \tag{2}$$

$$V = \frac{S}{cos(\theta)\ tan(\gamma)} \tag{3}$$

$$b = V\sqrt{1 + \cos^2(\theta)\tan^2(\gamma)} \tag{4}$$

For the unit cells with maximum height, $\theta = \gamma = \frac{\pi}{3}$ and $a = b = 3\ mm$. For the unit cells with minimum height, we set $\gamma = \frac{\pi}{9}$.

Results

In several tessellations, flat-foldability conditions based on Kawasaki's theorem were met which made them manufacturable by folding. Based on Kawasaki's theorem, a structure is flat-foldable if the sum of even and odd sequence of angles, each, equal to π. The tessellations which did not satisfy the Kawasaki's conditions were only modelled

numerically. Thanks to novel manufacturing technologies such as Additive Manufacturing such non-flat-foldable structures are now realizable [12]. The flat-foldable origamis namely checkered, linear X gradient, linear Y gradient, striped in the X direction, and striped in the Y direction provided twisting, local inflammation, bending, asp shape, and wavy deformations, respectively (Figure 2).

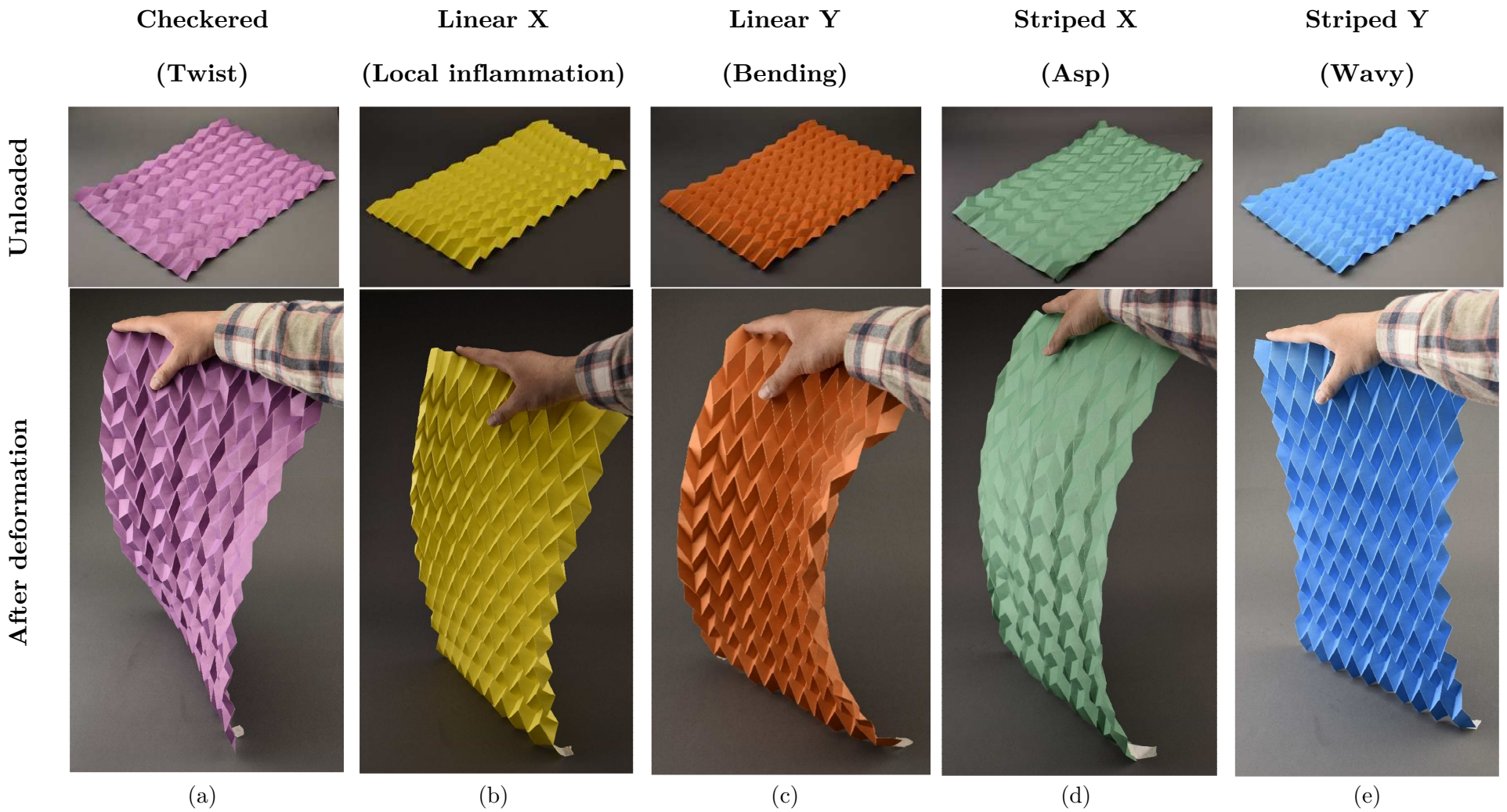

Figure 2: Deformation of (a) checkered, (b) linear X gradient, (c) linear Y gradient, (d) striped X, and striped Y tessellations.

The numerical results show that structures which depart (slightly or highly) from flat-foldability conditions namely concave radial gradient, convex radial gradient, linear X gradient (with variable mountain height), and striped X (with variable mountain height) distributions of unit cells show respectively saddle-shape, bending, combined twisting and bending, and combined wavy and bending deformations (Figure 3). Therefore, the results show that different proposed tessellation types are able to transform their shape into different 3D curvatures by means of in-plane incompatibilities. Overall, the achieved 3D curvatures from the nine proposed tessellations includ twisting, local inflammation, bending, asp-shape, wavy, saddle-shape, combined twisting/bending, and combined wavy/bending deformations (Figure 3). The maximum out-of-plane deformation in the checkered, linear X gradient (with variable unit cell width), linear Y gradient, striped X (with variable unit cell width), striped Y, concave radial gradient, convex radial gradient, linear X gradient (with variable mountain height), and striped X (with variable mountain height) structures are 19.9 mm, 4.5 mm, 9.4 mm, 4.7 mm, 2.1 mm, 8.8 mm, 11 mm, 14.9 mm, and 7.2 mm, respectively.

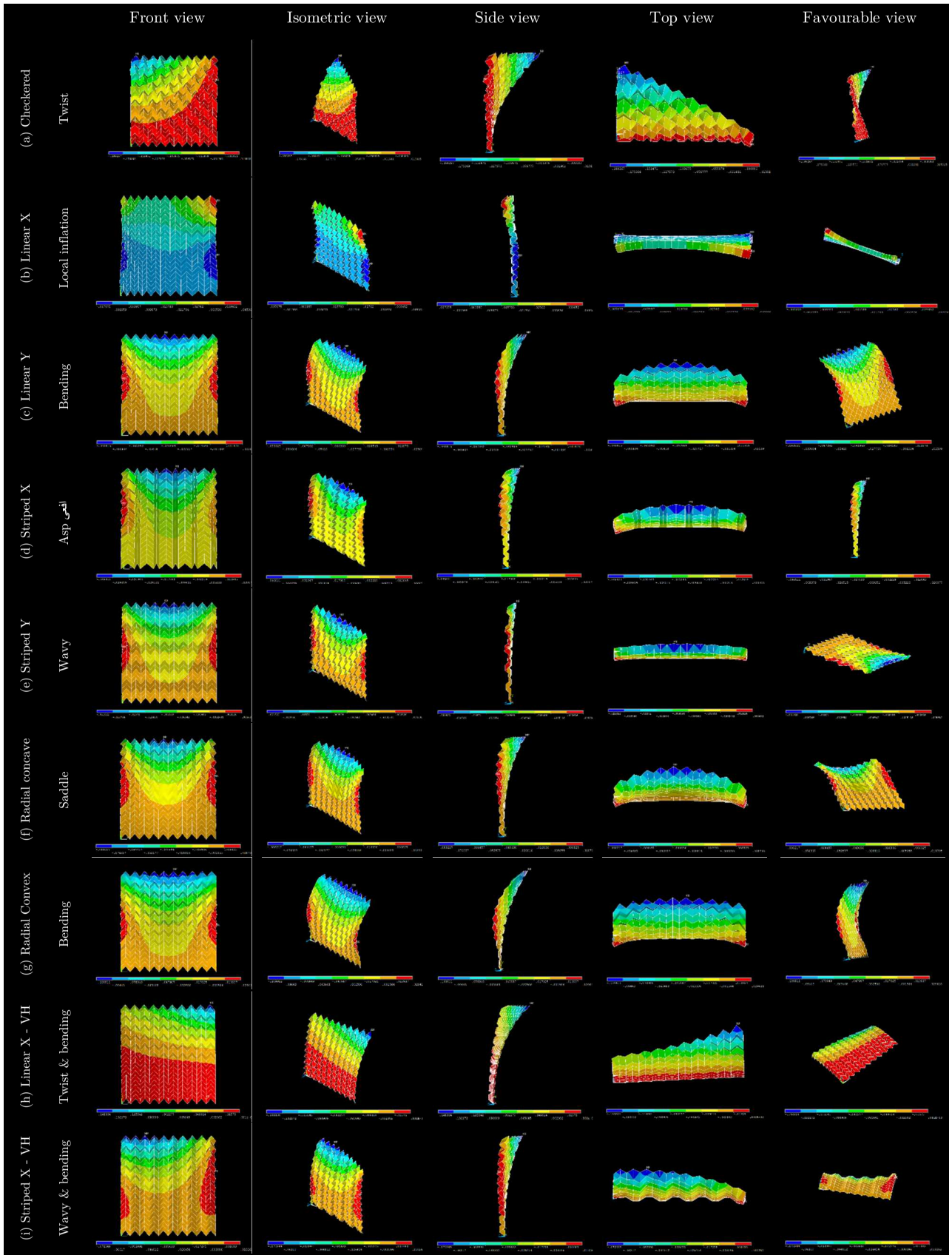
Front view
Isometric view
Side view
Top view
Favourable view
(a) Checkered
Twist
(b) Linear X
Local inflation
(c) Linear Y
Bending
(d) Striped X
Asp
(e) Striped Y
Wavy
(f) Radial concave
Saddle
(g) Radial Convex
Bending
(h) Linear X - VH
Twist & bending
(i) Striped X - VH
Wavy & bending

Figure 3: The curvatures resulting from Miura-ori origamis with (a) checkered, (b) linear X gradient (with variable unit cell width), (c) linear Y gradient, (d) striped X (with variable unit cell width), (e) striped Y, (f) concave radial gradient, (g) convex radial gradient, (h) linear X gradient (with variable mountain height), (i) striped X (with variable mountain height), and (j) regular distributions of unit cells. VH stands for variable (mountain) height.

Discussions

It is well known that flat-foldable origamis which have one degree of freedom are easily deployable and energy efficient. One way of making the non-flat foldable structures (Figure 3f-i) flat-foldable is to consider some holes in their structure and thus to transform the Miura-Ori origami structures into Mira-Ori hybrid origami-kirigami structures. Kirigami is a variation of origami that includes cutting in the sheet in addition to foldable crease lines. One such combination based on zig-zag strips was introduced in [13], and it was shown that such hybrid structures are flat-foldable.

Manipulation of Poisson's ratio, which was achieved by changing Miura-Ori characteristics spatially in this work, can be performed by other means to create similar 3D curvatures. As long as different regions of a flat plate are programmed to demonstrate different lateral behaviors upon receiving external stimulus, the plate would demonstrate curvatures similar to what was proposed in this study. Examples include plates with non-uniform/gradient distribution of thermal expansion coefficient under heat stimilus and plates with non-uniform swelling factor distribution under adjustable environmental (humidity and/or chemical) conditions. In fact, the mechanical actuation technique proposed in this study has the advantages of being inexpensive, easy to control, and mechanically durable.

As origamis are free from geometrical scales, the presented approaches can be generalized to other scales all the way from nano-scale to mega-structures. Therefore,

these configurations can have applications in several engineering devices such as robotics [14], self-folding assemblies [15], and self-morphing structures [16]. Such applications are more realizable due to recent advances in manufacturing technologies such as additive manufacturing [12], stress within thin films [17], nano-lithography [18], and small-scale hinge constructions [19, 20]. The actuation can be performed either globally or locally. Locally, the actuation can be done by making regions at the sides of each unit cell inflatable or stretchable to create respectively pressure or contraction at the two ends of each cell. This actuation mechanism can be compared to auto-stress phenomenon in organs [21]. Regardless of the actuation technique being local or global, each lattice structure deforms in such a way that it minimizes the total mechanical energy of the overall system [21]. This can cause different bifurcations such as local buckling, single curvature, or double curvature depending on the unit cell distribution (see Figure 2-3).

The other fact to mention is that the proposed designs can also be used in hinged configurations. In fact, we tried constructing such hinged assemblies (Figure 4). However, as the structures get larger and larger, and tessellation pattern numbers increase, the attention required to be paid to precision and accuracy increase exponentially. This is more pronounced in gradient assemblies. In case insufficient attention is paid to precision, very small inaccuracies in the placement of origami faces and attachment of the hinges can lead to very strong unwanted forces in sufficiently large structures. This not only decreases the robustness of the structure locally and as a whole, it also departs the structure from rigid-foldability, which, in turn, introduces unwanted energy-consumption through strain energy dissipation.

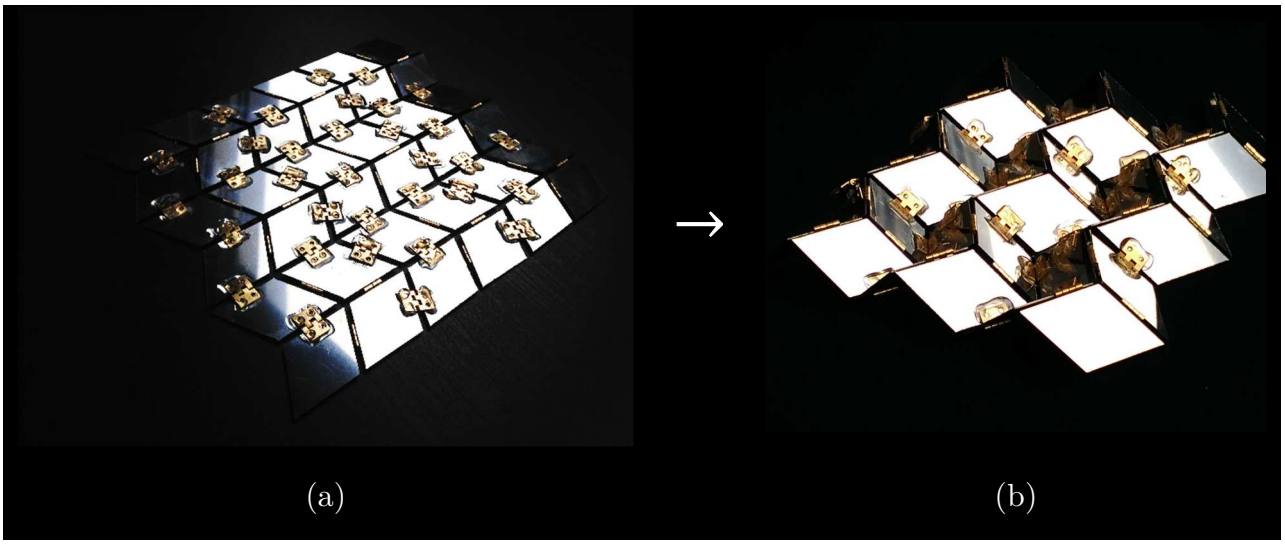

Figure 4: Hinged Miura-ori origami tessellation (a) before and (b) after folding

Finally, the basic gradient tessellations could be combined in dual or multiple configurations to give more complex shapes on demand. We have shown the benefits of such combinations in 2D gradient auxetic configurations for programming vase, barrel, and narrow-waisted shapes into the flat rectangular plates [10]. Combinations of the designs proposed in this study can be implemented to develop deformable surfaces such as flexible yet strong clothing, soft robotics, deformable batteries [22, 23], deformable electronics [24], and complex actuators [25]. Origami-based deformable electronics could demonstrate excellent performance of conventional rigid electrical components as well as high 3D deformability levels. The electronic performance in currently existing highly-deformable thin-film-based solutions are usually diminished to a high degree due to low areal coverage [23].

In summary, gradient Miura-ori origamis were introduced as a method to create out-of-plane curvatures. Nine types of unit cell distributions in Miura-ori origami lattice structure including checkered, linear gradient, concave radial gradient, convex radial gradient, and striped were considered. These distributions of Miura-ori origami led to several out-of-plane 3D curvatures with single- or double-curvatures such as twisting,

saddling, bending, local inflation, and wavy shapes, as well as their combinations when the origami lattice structure was loaded in compression in the direction parallel to the origami mid-plane. All the Gaussian curvatures (negative, positive, and zero) was achieved using the proposed models. Our approach will help tailoring complex pre-programmed surface geometries by employing basic gradient distributions of Miura-ori origami.

Methods

The specimens were generated from the original Miura-ori crease pattern. According to 3D models, creases were designed, transferred to papers, and folded by hand. Thin kraft papers (120 gsm) with thickness of 2.5 mm were used as initial flat sheets. All the specimens were made in one piece. All the fabricated origamis were placed vertically, and their lower edge was constrained using glue. The top side of the origami was compressed vertically manually for ≈ 2% strain (similar to the simulations).

ANSYS finite element (FE) modeling package was used to construct the geometry of the origami lattices and to carry out the simulations. An algorithm was developed to vary the unit cell height H or width S (Figure 1) depending on the type of tessellation. Each crease line was discretized using 10 elements. Therefore, each lattice structure consisted of 40,000 planar elements (SHELL 181 in ANSYS library). The material properties of Kraft 120 gsm paper was given to the models ($E_s = 1.7\ GPa$ and $\nu = 0.4$). The thickness of the origami was set to 2.5 mm. One side of each origami tessellation was constrained in the Y direction and the other side was compressed in the Y direction ($D_z = 6$ mm). The other degrees of freedom were kept free to allow out-of-plane displacements. 10×10 tessellations were used for all the computational models.

References

1. Mohammadi, K., M. Movahhedy, I. Shishkovsky, and R. Hedayati, *Hybrid anisotropic pentamode mechanical metamaterial produced by additive manufacturing technique* Applied Physics Letters, 2020. **117**(6): p. 061901.
2. Hedayati, R., S.J. Salami, Y. Li, M. Sadighi, and A. Zadpoor, *Semianalytical geometry-property relationships for some generalized classes of pentamodelike additively manufactured mechanical metamaterials.* Physical Review Applied, 2019. **11**(3): p. 034057.
3. Silverberg, J.L., A.A. Evans, L. McLeod, R.C. Hayward, T. Hull, C.D. Santangelo, and I. Cohen, *Using origami design principles to fold reprogrammable mechanical metamaterials.* science, 2014. **345**(6197): p. 647-650.
4. Mahadevan, L. and S. Rica, *Self-organized origami.* Science, 2005. **307**(5716): p. 1740-1740.
5. Shyer, A.E., T. Tallinen, N.L. Nerurkar, Z. Wei, E.S. Gil, D.L. Kaplan, C.J. Tabin, and L. Mahadevan, *Villification: how the gut gets its villi.* Science, 2013. **342**(6155): p. 212-218.
6. Dudte, L.H., E. Vouga, T. Tachi, and L. Mahadevan, *Programming curvature using origami tessellations.* Nature materials, 2016. **15**(5): p. 583.
7. Kolken, H.M. and A. Zadpoor, *Auxetic mechanical metamaterials.* RSC advances, 2017. **7**(9): p. 5111-5129.
8. Liu, K., T. Tachi, and G.H. Paulino, *Invariant and smooth limit of discrete geometry folded from bistable origami leading to multistable metasurfaces.* Nature communications, 2019. **10**(1): p. 1-10.
9. Wei, Z.Y., Z.V. Guo, L. Dudte, H.Y. Liang, and L. Mahadevan, *Geometric mechanics of periodic pleated origami.* Physical review letters, 2013. **110**(21): p. 215501.
10. Hedayati, R., M. Mirzaali, L. Vergani, and A. Zadpoor, *Action-at-a-distance metamaterials: Distributed local actuation through far-field global forces.* APL Materials, 2018. **6**(3): p. 036101.
11. Schenk, M. and S.D. Guest, *Geometry of Miura-folded metamaterials.* Proceedings of the National Academy of Sciences, 2013. **110**(9): p. 3276-3281.
12. Harris, J. and G. McShane, *Metallic stacked origami cellular materials: Additive manufacturing, properties, and modelling.* International Journal of Solids and Structures, 2020. **185**: p. 448-466.
13. Eidini, M., *Zigzag-base folded sheet cellular mechanical metamaterials.* Extreme Mechanics Letters, 2016. **6**: p. 96-102.
14. Hawkes, E., B. An, N.M. Benbernou, H. Tanaka, S. Kim, E.D. Demaine, D. Rus, and R.J. Wood, *Programmable matter by folding.* Proceedings of the National Academy of Sciences, 2010. **107**(28): p. 12441-12445.
15. Janbaz, S., R. Hedayati, and A. Zadpoor, *Programming the shape-shifting of flat soft matter: from self-rolling/self-twisting materials to self-folding origami.* Materials Horizons, 2016. **3**(6): p. 536-547.

16. Paik, J.K., A. Byoungkwon, D. Rus, and R.J. Wood. *Robotic origamis: Self-morphing modular robot.* in *ICMC*. 2012.
17. Shenoy, V.B. and D.H. Gracias, *Self-folding thin-film materials: From nanopolyhedra to graphene origami.* Mrs Bulletin, 2012. **37**(9): p. 847-854.
18. Matković, A., B. Vasić, J. Pešić, J. Prinz, I. Bald, A.R. Milosavljević, and R. Gajić, *Enhanced structural stability of DNA origami nanostructures by graphene encapsulation.* New Journal of Physics, 2016. **18**(2): p. 025016.
19. Kuribayashi, K., K. Tsuchiya, Z. You, D. Tomus, M. Umemoto, T. Ito, and M. Sasaki, *Self-deployable origami stent grafts as a biomedical application of Ni-rich TiNi shape memory alloy foil.* Materials Science and Engineering: A, 2006. **419**(1-2): p. 131-137.
20. Overvelde, J.T., T.A. De Jong, Y. Shevchenko, S.A. Becerra, G.M. Whitesides, J.C. Weaver, C. Hoberman, and K. Bertoldi, *A three-dimensional actuated origami-inspired transformable metamaterial with multiple degrees of freedom.* Nature communications, 2016. **7**(1): p. 1-8.
21. Moulia, B., *Leaves as shell structures: double curvature, auto-stresses, and minimal mechanical energy constraints on leaf rolling in grasses.* Journal of Plant Growth Regulation, 2000. **19**(1): p. 19-30.
22. Zhang, Y., Y. Huang, and J.A. Rogers, *Mechanics of stretchable batteries and supercapacitors.* Current Opinion in Solid State and Materials Science, 2015. **19**(3): p. 190-199.
23. Song, Z., T. Ma, R. Tang, Q. Cheng, X. Wang, D. Krishnaraju, R. Panat, C.K. Chan, H. Yu, and H. Jiang, *Origami lithium-ion batteries.* Nature communications, 2014. **5**(1): p. 1-6.
24. Song, W.J., S. Yoo, G. Song, S. Lee, M. Kong, J. Rim, U. Jeong, and S. Park, *Recent progress in stretchable batteries for wearable electronics.* Batteries & Supercaps, 2019. **2**(3): p. 181-199.
25. Martinez, R.V., C.R. Fish, X. Chen, and G.M. Whitesides, *Elastomeric origami: programmable paper-elastomer composites as pneumatic actuators.* Advanced functional materials, 2012. **22**(7): p. 1376-1384.